Measuring the Validity of Sensing Coverage in the Presence of Anchor Misplacement

Yaser Al Mtawa
School of Computing,
Queen's University
Kingston, Ontario K7L 2N8
Canada
Email: yalmtawa@cs.queensu.ca

Hossam S. Hassanein
School of Computing,
Queen's University
Kingston, Ontario K7L 2N8
Canada
Email: hossam@cs.queensu.ca

Nidal Nasser
College of Engineering
Alfaisal University
Riyadh, 11533
Saudi Arabia
Email: nnasser@alfaisal.edu

Abstract*— *In the Era of the Internet of Things (IoT) the validity of sensing coverage is of utmost importance as it affects the reliability of sensing services. The presence of anchor misplacement poses a challenge on the validity of sensing coverage. This kind of challenge has generally been overlooked in sensing coverage research. In this paper, we investigate the sensing validity under several scenarios of anchor misplacement with different displacement values. We also investigate the error components of measurement and anchor misplacement, and their resultant impact on sensing validity. We model the problem using computational geometry. We provide a theoretical approach to test such validity. Then we propose an algorithm that implements the suggested approach. Our results are further validated through extensive simulation. This study shows interesting results that could be used to mitigate the negative impact anchor misplacement has on sensing coverage.

Keywords— Anchor Misplacement, Wireless Sensor Networks, Internet of Things, Sensing Coverage, Intra-Triangle Coverage, Triangulation.

I. Introduction

The coverage problem is considered an important measurement of the quality of a sensor network. It measures to what extent the sensor network can monitor the surrounding physical space. Sensing coverage in wireless sensor networks has attracted much research. The requirements of sensing coverage vary according to the application. The majority of sensing coverage research assumes that the anchor nodes are in the correct positions and, therefore, do not pose an error component on the localization of sensing nodes. For example, in [1] the authors propose an approach for anchor misplacement to achieve optimal localization with a minimum number of deployed anchors. They assume that the anchor nodes will be placed precisely in their correct position. Taking into consideration anchor misplacement, the analytical results of their research will definitely be different. The authors of [2] provide a closed formula for equilateral triangle grid-based deployment that achieves full coverage with a minimum number of sensors and tolerates the anchor sensor misplacement.

Misplaced anchor nodes pose different error magnitudes on affected sensing nodes according to the displacement value and the distance between the misplaced anchor node and the sensing node. If some anchor nodes were inaccurately positioned, many of the sensing reports will be invalid. In this research, we investigate the sensing validity in the presence of anchor misplacement with and without the existence of measurement errors. Given a set of anchors, if some of them are misplaced, can we measure the validity of the sensing reports of each sensing node? One interesting aspect of this research is that it addresses the validity of sensing reports in the presence of anchor misplacement in a non-uniform sensing area which represents either a convex or concave set.

Measurement error and set up error are examples of error components that affect IoT services. In this paper we: 1) formulate the problem of validity of sensing coverage reports; 2) utilize triangulation tool to provide theoretical analysis for sensing coverage problem that have been formed as a result of anchor misplacement; 3) develop an efficient algorithm to test the validity of sensing reporting; and 4) implement the algorithm and run various experiments to show the correctness of our theoretical analysis. To the best of our knowledge, this is the only research that measures the sensing validity in the presence of anchor misplacement. In this research, we use the terms "sensing node" and "sensing object" interchangeably.

II. Motivation and Related Work

Assume an experiment is being conducted to measure the air temperature and humidity levels in a warehouse. The warehouse is divided into small non-uniform areas in which sensing nodes are intended to monitor these individual areas as shown in Fig. 1. For this purpose, heterogeneous sensors that are already deployed in all areas will be used. Each sensing node was placed in its "residence" area within the warehouse. So the residence area of a sensing node s_i is the area of the warehouse where s_i is supposed to monitor. Several anchor nodes were misplaced or had inaccurate locations, the goal is to measure whether or not the sensing nodes still convey accurate reports. This tests whether or not the estimated location of each sensing node is still within its "residence" area.

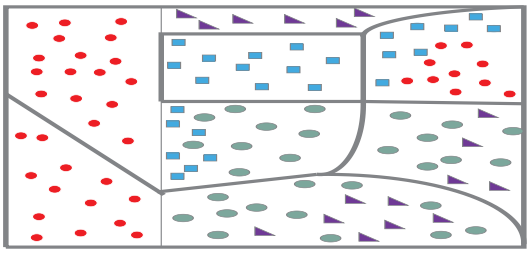

Fig. 1 Non-uniform sensing region with multiple sensing providers.

978-1-4673-8999-0/17/$31.00 ©2017 IEEE

Existing work on sensing coverage in WSNs assumes sensors are homogeneous and belong to only one sensing service provider. Most of the research addresses deterministic sensor placement and deployment planning to achieve greater coverage and/or to extend the network lifetime [3]. The sensing coverage problem is more pronounced in the IoT context due to the critical challenges of scalability, robustness, heterogeneity, and security [4] as a consequence of the explosive growth of a number of devices with different technologies being spread over a large terrain. It is predicted that IoT will consist between 15-20 billion smart objects by 2020 [5].

The challenge in this setting is the reliability of sensing reports. Our previous work [6] shows that anchor misplacement degrades localization accuracy. Sensing coverage quality is also affected due to invalidity of data collection as the sensed data may contain erroneous locations if their corresponding sensor nodes were localized inaccurately using misplaced anchor nodes, and by inefficient energy consumption as the sensor's battery becomes drained quickly due to inaccurate decision of routing protocol based on inaccurate locations of sensing nodes [7]. In [8], the coverage hole problem in IoT context is investigated. The work identifies each coverage hole, finds its location, and calculates the inner and outer bounds of its area size. In this paper, the validity of sensing coverage in the presence of anchor misplacement and how to measure it is addressed.

III. Problem Description and System Model

We first introduce the necessary definitions and assumptions. The definition of sensing coverage in [8] is adopted in this research.

Definition 1: Let s_i be a sensing object with an unknown location. Let s_i belong to a "residence" sensing area A_k. Then sensing report of s_i is valid (or true positive (TP)) if the estimated location of s_i is still within A_k. Otherwise, it is invalid (or true negative (TN)) as the estimated location of s_i is outside of A_k.

Given a random deployment of sensing nodes in a non-uniform sensing field, and a localization error posed by anchor misplacement and measurement error on some sensing nodes, we are interested in investigating and modeling the problem of measuring the validity of sensing reporting which depends on the estimated location of the affected sensing nodes. In particular, we are interested in classifying the set of sensing nodes into true positive (TP), i.e., "valid", or true negative (TN) i.e., "invalid", sensing reports. The main assumptions are the following:

1. Localization of sensing objects is multi-lateration based with minimum mean squared error (MMSE) for fine-tuning the estimated positions.
2. Anchor misplacement and measurement error are the most critical sources of error that leads to localization uncertainty (i.e., disregarding other sources of error).

We adopt the same network and sensing models in [8], with random sensor deployment and binary disk sensing model.

IV. Modeling Sensing Area

Grid-based deployment of sensing objects provides straight forward analysis of the problem of sensing coverage. For example, [2] provides a closed form of the number of sensing nodes and the spaces between them under equilateral-triangle grid deployment. This is not the case in random deployments where the sensing region has non-uniform areas.

Our approach depends on creating a polygon to represent each sensing area as shown in Fig. 2 where the different coloured shapes denote the estimated positions of heterogeneous sensing nodes. The region bounded by gray line represents the sensing area. In order to test the location of each sensing node, the representative inner polygon is triangulated. Then we apply a cross product technique to assess the presence of a point inside a triangle. Consequently, the sensing node s_i is either a true positive (TP) if it is inside any triangle, or a true negative (TN) otherwise. Next, we discuss how to create the inner polygon for each sensing area. Then the level of granularity to test the validity of sensing reporting will be addressed.

A. *Modeling Non-Uniform Sensing Area*

The deployment of sensing nodes usually creates a non-uniform sensing area. Measuring sensing coverage, in this case, is not a straightforward generalization as in its uniform counterpart. We assume that the border of each area that has a sensing node is known. This means we know the points on this border. Our goal is to detect whether or not the location of the sensing nodes affected by anchor misplacement are still within the residence sensing area. We model each sensing area as a simple polygon. We select the polygon to be strictly inscribed inside the sensing area (i.e., inner polygon). The question arises here is how do we compute such a polygon? Before answering this question, we should first illustrate the granularity related to sensing report. It is intuitive that the granularity will be finer if more points are selected from the border of the sensing area to be vertices in the computed polygon. Finer granularity of the sensing area provides more accurate decisions regarding the validity of sensing coverage. Without loss of generality we assume that the sensing area is a convex set, hence its associated polygon is convex as well. Assume the level of granularity is determined, we choose randomly the vertices that represent the edges of each sensing area. Then we connect these vertices clockwise to form an associated polygon.

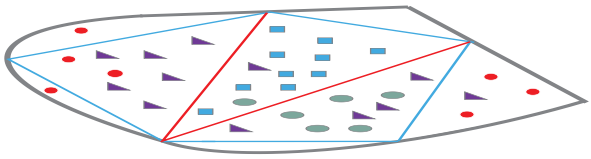

Fig. 2 A Possible inner polygon with a triangulation as a model of a non-uniform sensing area.

B. *The Impact of Error Components on Sensing Validity*

Here we study the error components that impact the localization accuracy and, consequently, affect the ratio of valid

sensing reports. It is logical to address error components such as anchor misplacement and measurement error which inherently affects the estimated positions of sensing nodes. Unlike measurement error, which impacts the localization accuracy of all sensing nodes, anchor misplacement affects only the sensing nodes in the vicinity of misplaced anchor nodes. Therefore, the differentiation between the impact of both error components is required. To achieve this, we need to know to what extent anchor misplacement contributed to the status of the sensing report of each affected sensing node. We assume there is a measurement error model which is not changed through time and can be established prior to network deployment. In this research, two error-force vectors (EFVs), namely measurement and misplacement vectors are considered. Let $EFV_{meas}(s_i)$, $EFV_{misp}(s_i)$ and $EFV_{result}(s_i)$ denote the error-force of mesurement, misplacement, and resultant vectors, respectively. $EFV_{result}(s_i)$ is the vector sum of $EFV_{meas}(s_i)$ and $EFV_{misp}(s_i)$ exerted during the localization of s_i as shown in Fig. 3. disregarding other less important error components, we have the following formula:

$$\left|EFV_{meas}(s_i) + EFV_{misp}(s_i)\right| = \sqrt{(x - x_i)^2 + (y - y_i)^2} \quad (1)$$

where |.| denotes the magnitude of a vector, (x, y) and (x_i, y_i) are the actual and estimated location of sensing node s_i , respectively. Furthermore, let $C_{meas}(s_i)$, $C_{misp}(s_i)$ denote the magnitudes of contributed components of measurement and misplacment error, respectively, on the resultant error vector of sensing node s_i. Assume that each sensing node stores the values of $C_{meas}(s_i)$ and $C_{misp}(s_i)$. Note that if the two force vectors are in different directions (i.e., the angle between them is greater than $\frac{\pi}{2}$), then the smaller out of $C_{meas}(s_i)$ and $C_{misp}(s_i)$ should have a negative sign.

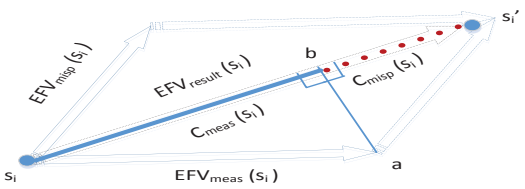

Fig. 3 Contributed errors of measurement and misplacement components in total resultant error.

Next, we conduct an experiment to show the impact of $C_{meas}(s_i)$ and $C_{misp}(s_i)$ on Root Mean Square Distance (RMSD). RMSD is widely used in literature as an indicator of estimation error in different localization algorithms [6]. Anchor misplacement could be random or ordered. Likewise, anchor displacement value could be random or fixed. Therefore, there are four different combinations of anchor misplacement and displacement values:1) ordered anchor misplacement with fixed displacement value (OM-FD), 2) random anchor misplacement with fixed displacement value (RM-FD), 3) ordered anchor misplacement with random displacement (OM-RD), and 4) random anchor misplacement with random displacement value (RM-RD). In Fig. 4, it is interesting to see that the deployment setting of RM-RD provides the least value of average RMSD among all other deployment settings. This interesting result supports the results in [9] where the authors found that random measurement contributes to high accuracy. Our results provide an extra finding that even with no measurement error, RM-RD provides higher localization accuracy. It is intuitive to see that RMSD values gets smaller as Signal to Noise Ratio (SNR) values gets bigger because the impact of measurement error gets smaller as well. Furthermore, the figure show that the impact of $C_{misp}(s_i)$ on accuracy becomes less effective as measurement error gets higher. We can conclude that RMSD is not so sensitive to anchor misplacement in high measurement-error environment because $C_{misp}(s_i)$ gets smaller compared to $C_{meas}(s_i)$ as $EFV_{meas}(s_i)$ cancels the effect of $EFV_{misp}(s_i)$.

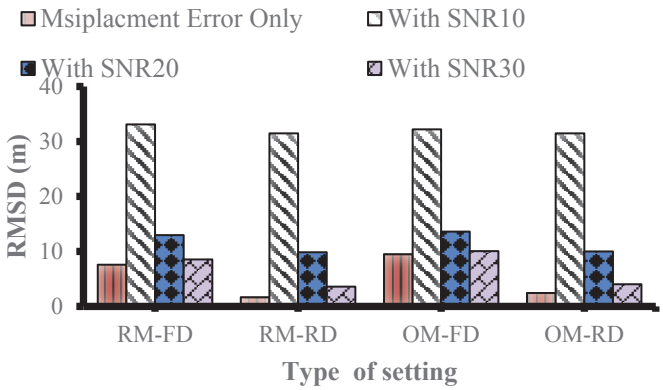

Fig. 4 The impact of the four different settings on RMSD (fixed displacement is set to 10m, random displacement follows $N(0,10)$, RMSD is averaged over 14 misplaced anchor nodes)

C. *Intra-Triangle Boundary Testing*

By using the computational geometry tool of triangulation, a representative polygon is triangulated. Suppose there is a set $\mathcal{A} = \{A_1, A_2, \ldots, A_k\}$ of sensing areas. The representative polygon of each of these sensing areas will be divided into triangles as shown in Fig. 2. Then we check whether or not the position of a sensing node resides within any of these triangles. This is referred to as intra-triangle testing. As a result, there are two possible residence places of an estimated position. The first possible place (R1), the estimated position is inside one of the polygon's triangles which means TP sensing node. The second place (R2), the estimated position is outside all the polygon's triangles which means TN sensing node. Note that, when an estimated position of a sensing node s_i resides in R2, this means that the magnitude of $EFV_{result}(s_i)$ becomes large enough and, hence, localize s_i outside of its residence sensing area. Consequently, the accuracy of the sensing validity becomes lower. On the other hand, if the sensing nodes reside in R1, this means that the magnitude of $EFV_{result}(s_i)$ has no tangible impact on sensing quality. The following definition formalizes our discussion about intra-triangle testing.

Definition 2: Let area $A_1 \in \mathcal{A}$ be a sensing area and P_{A_1} be its representative polygon. Furthermore, let $S_{A_1} = \{s_1, s_2, \ldots, s_k\}$ be a set of sensing nodes deployed in area A_1, where k is the number of sensing nodes in A_1 . Moreover, let $T_{A_1} = \{T_1, T_2, \ldots, T_l\}$ be the set of triangles of P_{A_1}. We denote intra-triangle testing to the test that evaluates whether or not an

estimated location of sensing node $s_i \in S_{A_1}$ resides inside any triangle of T_{A_1}.

To check the inclusion of a point inside a triangle, we follow the cross product method. Fig. 5 shows a triangle ABC and a point s_i' inside it. Let $\overrightarrow{AC}$ denote the vector that starts at point A and is directed towards point C. The idea behind cross product method is that the point is inside ABC only if s_i' above vector BC, left to vector AC, and right to vector AB. If any one of these conditions fails, the point is outside the triangle. The direction of cross product of AC and As_i' should be in the same direction of the cross product of AC and AB as in Fig. 5. The remaining combinations of vectors can be tested in similar way (see Algorithm 1).

Algorithm 1: Point in a Triangle *(PIaT)*

Input: s_i', T_i; // point s_i' and a triangle T_i

Output: Boolean value; //return true of a point s_i' resides in a triangle T_i. Otherwise, return false.

$\{A,B,C\}$ = *get_Vertices*(T_i);// return $T_i's$ vertices

$$if\,(\,has\_similar\_dir\left(\left(\overrightarrow{AC}\times\overrightarrow{As_i'}\right),\left(\overrightarrow{AC}\times\overrightarrow{AB}\right)\right)\,\&\&$$
$$has\_similar\_dir\left(\left(\overrightarrow{BC}\times\overrightarrow{Bs_i'}\right),\left(\overrightarrow{BC}\times\overrightarrow{BA}\right)\right)\,\&\&$$
$$has\_similar\_dir\left(\left(\overrightarrow{AB}\times\overrightarrow{As_i'}\right),\left(\overrightarrow{AB}\times\overrightarrow{AC}\right)\right))$$

{ *return true*} *else return false;*

The particulars of the functions in PIaT are as follows: Function *get_Vertices*(T_i) takes a triangle as an input and return the set of vertices of T_i. Function $has\_similar\_dir(\vec{v},\vec{u})$ tests whether or not vectors $\vec{v}$ and $\vec{u}$ have the same direction. $has\_similar\_dir$ returns true if the dot (i.e., inner) product of $\vec{v}$ and $\vec{u}$ is nonnegative. Otherwise, it returns false.

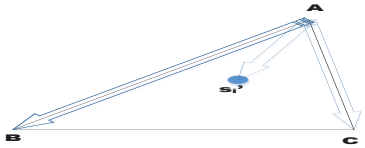

Fig. 5 Test a point in a triangle by cross-product method.

D. Validity Check Algorithm

The following algorithm tests the validity of sensing reports of a misplacement-affected sensing node.

Algorithm 2: *Testing Validity of the Sensing Report(TVSR)*

Input: T_{A_1}, S_{A_1} /*Set of triangles of a representative polygon of area A_1 and a set of sensing nodes in A_1, respectively*/

Output: Classified sensing nodes as TP, or TN.

For each triangle $T_i \in T_{A_1}$
  For each sensing node $s_i \in S_{A_1}$
    If (*PIaT*(s_i', T_i)) then {
      // s_i' is the estimated position of s_i
      set_Intra-Triangle_sensing(s_i', T_i) = 1;
    }// end if
  End For;
End For;
For each sensing node $s_i \in S_{A_1}$
  If(Intra-Triangle_sensing(s_i') == 1){
    setValidSensing = *setValidSensing* $\cup \{s_i\}$
  }*Else* {
    setInvalidSensing = *setInvalidSensing* $\cup \{s_i\}$}
End For;

TVSR algorithm takes two sets: triangulation set (T_{A_1}) of a representative polygon of area A_1 and a set S_{A_1} of sensing nodes in A_1. The output is two classes of sensing nodes: TP or TN. In the first two loops, the algorithm tests the inclusion of each sensor's location point in every triangle of T_{A_1}. If such a triangle is found, the sensing node is added to TP class. The next loop marks as TN all the remaining sensing nodes that are not TP. The specifications of the functions are as follows: *PIaT*(s_i', T_i) calls PIaT algorithm with two arguments, namely a point and a triangle. It returns true if s_i' resides inside T_i. Otherwise, it returns false. *set_Intra-Triangle_sensing*(s_i', T_i) =1 marks point s_i' as TP. The rest of the sensing nodes are marked as TN.

V. NUMERICAL RESULTS AND DISCUSSION

We use NS-3 to simulate different scenarios of the conducted experiments. The outputs of the simulation step will be inputs for a Visual Studio C++ program which includes our implementation of the proposed algorithm. We also utilize the implementation of a distributed algorithm in [10] to construct a triangulation. The experiments show the effect of the following parameters on the percentage of valid and invalid sensing reports: the number of misplaced anchor nodes, and the measurement error component (i.e., $EFV_{meas}(s_i)$). We assume that $EFV_{meas}(s_i)$ follows a normal distribution with mean zero and variance ${\sigma_{i,j}}^2$, where i and j are the identifications of the sensing and anchor nodes, respectively. In order to better estimate the distance between the sensing and anchor nodes, we follow the formulation in [11] which had adopted the following equation for the variance: ${\sigma_{i,j}}^2 = \frac{{d_{i,j}}^2}{SNR}$, where SNR is signal-to-noise ratio. The parameters of all experiments are set as follows, unless otherwise stated. The terrain is a square of 200 × 200 m^2. The terrain is a warehouse which is divided into six non-uniform sensing areas marked A_1-A_6, see Fig. 6. However, for the sake of simplicity and to avoid repetition, we will only focus on sensing area A_1. The number of sensor and anchor nodes per sensing area are 30 and 4, respectively. The sensing nodes are deployed randomly in each sensing area while the anchor nodes are placed on the corners of each sensing area. They are numbered 1-14. For full communication coverage, the transmission range is set to be 142m which is equivalent to half of the diameter of the terrain. As we illustrated in Section IV(B), there are two options for anchor misplacement: ordered or random. Under ordered misplacement, the anchor nodes begin to be misplaced in order starting from anchor node number 1, then anchor node number 2, and so on until reaches the required number of misplaced anchor nodes. The random anchor misplacement follows a uniform random distribution. Similarly, the displacement value of misplaced anchor nodes can be either fixed or random. The fixed displacement value is set to 10m on both x- and y-coordinates. In the case of random displacement value, the

displacement value follows a normal distribution on both x- and y-coordinates with mean zero and variance of 10m. The results of all conducted experiments are calculated based on the average of 10 runs.

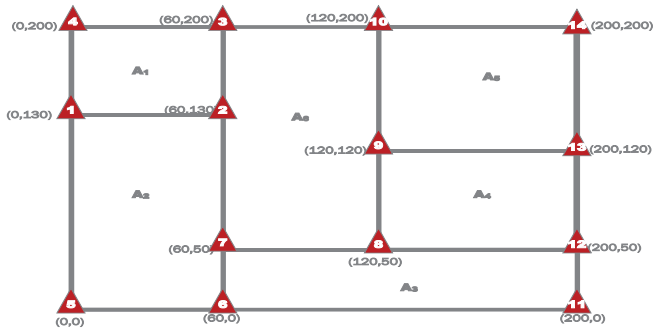

Fig. 6 Warehouse model with six non-uniform sensing areas with 14 numbered anchor nodes placed in the corners

We first study the impact of measurement error on sensing validity. The number of misplaced anchor nodes in this experiment is set to 5. The SNR values are 10, 20, and 30 db. Furthermore, ordered anchor misplacement with fixed displacement value (OM-FD) is adopted in this scenario. The percentage of TP and TN of the sensing nodes will be calculated in two cases: with and without the existence of measurement error (i.e., SNR-Free). The results are shown in Fig. 7. The results show that as the measurement error becomes smaller, the percentage of TP increases while the percentage of TN decreases. On the other hand, TP-SNR-Free and TN-SNR-Free indicates to the other case where no measurement error is applied. We note that the percentage of TP is at least as three times as percentage of TN sensing nodes. Furthermore, Fig. 7 shows that TP-SNR-Free and TN-SNR-Free tend to be convergence limits for TP, and TN, respectively. This is because, as the SNR value gets higher, the impact of C_{meas} gets smaller which makes the resultant error component more driven by C_{misp} .

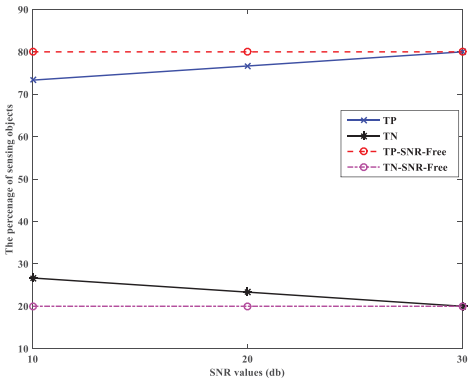

Fig. 7 The impact of measurement error on the sensing validity

Next we study the impact of anchor misplacement on sensing validity under OM-FD setting. We conduct this experiment under various values of SNR, namely, 10, 20, and 30 db. The results are shown in Fig. 8.

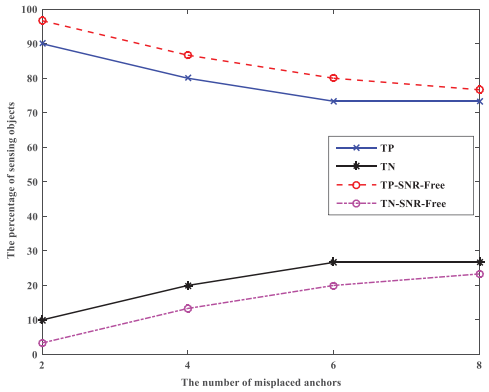

(a) SNR=10 db

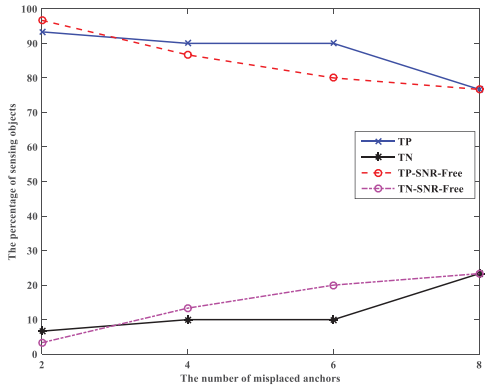

(b) SNR=20 db

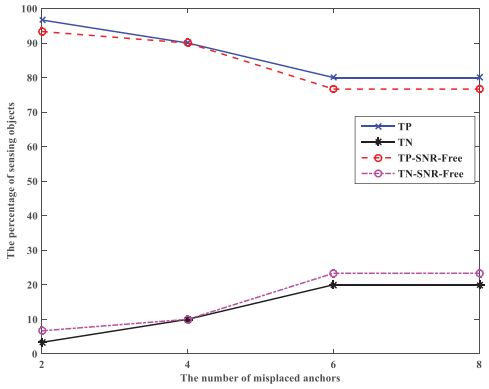

(c) SNR=30 db

Fig. 8 The impact of anchor misplacement on sensing validity under OM-FD with different values of SNR.

The graph in Fig. 8 shows that as the number of misplaced anchor nodes increases, the percentage of TP decreases, while the percentage of TN increases for all SNR values. Fig. 8 (a) has the lowest percentage of TP sensing nodes with average 70%, compared to 77% and 80% in Fig. 8(b) and (c), respectively. It is intuitive to see that while the SNR value increases, TP converges to TP-SNR-Free, and TN converges to TN-SNR-Free. This is because C_{meas} becomes smaller and eventually will have trivial values compared to C_{misp}.

The third experiment is similar to the previous one. However, it is conducted under RM-RD setting. For the sake of space, we only include the result for SNR value of 10.

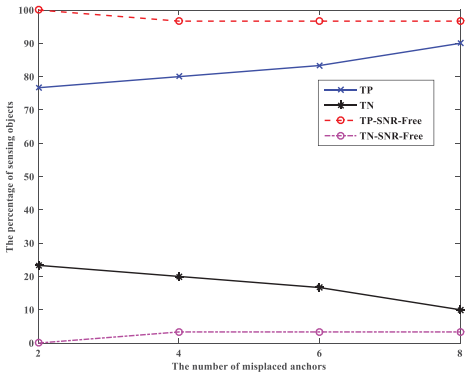

Fig. 9 The impact of anchor misplacement on sensing validity under SNR 10.

Fig. 9 shows interesting results where the number of misplaced anchors has no negative impact of sensing validity. In contrary, as the number of misplaced anchor nodes increases, the percentage of TP sensing nodes increases while the percentage of TN sensing nodes decreases. This means that measurement error cancels out the impact of anchor misplacement.

Lastly, we compare the impact of the four combinations that we listed in Section IV(B). In this experiment, the TP, TN, TP-SNR-Free and TN-SNR-Free values are averaged over 14 misplaced anchor nodes.

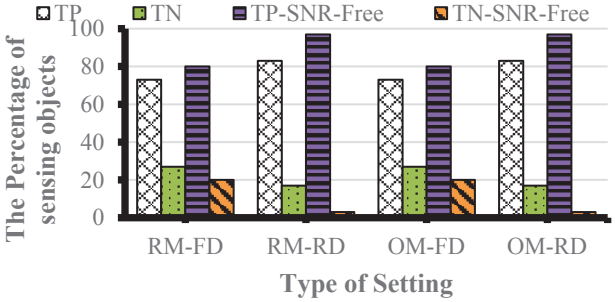

Fig. 10 The impact of different settings on sensing validity

The results show that the best percentage values of valid sensing are obtained when the anchor displacement values are selected randomly, see Fig. 10. The differences between TP, TN and their SNR-Free counterparts are expected to get smaller when the values of SNR increases. This is because the measurement error gets smaller and, hence, converge to SNR-Free case.

VI. Concluding Remarks

In this paper, we invistigate the problem of sensing validity under the presence of anchor misplacement with and without the existence of measurment error. We present an algorithm that tests the sensing validity and classifies the snesing nodes as true positive or true negative. The results of our research show the importance of validating the sensing reports especially under the presence of error components such as anchor misplacement and measurement error. Results also show the need to evaluate the impact of anchor location uncertainty on the performance of the existing coverage protocols. While collective IoT sensors improves the percentage of sensing coverage, anchor misplacement increases the TN sensing nodes. The findings of our study also show that the randomness of anchor misplacment and displacment value mitigates the impact of anchor misplacment and gets higher valid sensing rate. Furthermore, our findings suggest that low SNR values undermines the impact of anchor misplacement. Under high SNR values, extending the sensing range of the affected sensing nodes reduces the impact of anchor misplacement and provide a great number of valid sensing report.

Acknowledgement

This research is supported by a grant from the Natural Sciences and Engineering Research Council of Canada (NSERC) under grant number: CRDPJ445517.

References

[1] N. Lasla, M. Younis, A. Ouadjaout, and N. Badache, “On optimal anchor placement for efficient area-based localization in wireless networks,” in *2015 IEEE International Conference on Communications (ICC)*, 2015, pp. 3257–3262.

[2] G. Takahara, K. Xu, and H. Hassanein, “Efficient Coverage Planning for Grid-Based Wireless Sensor Networks,” in *IEEE International Conference on Communications, 2007*, pp. 3522–3526.

[3] N. Ahmed, S. S. Kanhere, and S. Jha, “The Holes Problem in Wireless Sensor Networks: A Survey,” *SIGMOBILE Mob. Comput. Commun. Rev.*, vol. 9, no. 2, pp. 4–18, Apr. 2005.

[4] S. M. A. Oteafy and H. S. Hassanein, “Resource Re-use in Wireless Sensor Networks: Realizing a Synergetic Internet of Things,” *Journal of Communications*, vol. 7, no. 7, Jul. 2012.

[5] H. Zhang, “Planet of the things,” *Computer Fraud & Security*, vol. 2016, no. 3, pp. 16–17, Mar. 2016.

[6] Y. Al Mtawa, N. Nasser, and H. Hassanein, “Mitigating Anchor Misplacement Errors in Wireless Sensor Networks,” *IEEE International Wireless Communications & Mobile Computing*, pp. 569-575, Oct. 2015.

[7] Y. Al Mtawa, H. Hassanein, and N. Nasser, “The Impact of Anchor Misplacement on Sensing Coverage,” *IEEE Wireless Communications and Networking*, pp. 1-7, April 2016.

[8] Y. Al Mtawa, H. Hassanein, and N. Nasser, “Identifying Bounds on Sensing Coverage Holes in IoT Deployments,” *IEEE Global Communications*, pp. 1-6, Dec. 2015.

[9] E. J. Candes and T. Tao, “Decoding by linear programming,” *IEEE Transactions on Information Theory*, vol. 51, no. 12, pp. 4203–4215, Dec. 2005.

[10] “Delaunay Triangulation Library for C++,” 2014. [Online]. Available: http://www.geom.at/fade2d/html/. [Accessed: 03-Oct-2015].

[11] W. M. Ibrahim, H. S. Hassanein, and A. E. M. Taha, “Does multi-hop communication enhance localization accuracy?,” in *2013 IEEE Global Communications*, 2013, pp. 121–126.